Asian Journal of Agriculture and Biology
https://doi.org/10.35495/ajab.2024.193

Original Article

Potential toxicity and mechanistic insights into organ-specific damage induced by iron oxide nanoparticles in *Oryctolagus cuniculus*

Muhammad Shahid Khan[1], Tariq Hussain[2], Saeed Ahmad Buzdar[3], Muhammad Raza Hameed[4], Muhammad Taslim Ghori[5], Aliza Maheen[6], Nadeem Ali[7], Beenish Imtiaz[8], Muhammad Rafi Qamar[5], Ahmed Saleh Summan[9], Arooj Ali[3*], Rashid Iqbal[10], Riaz Hussain[11*]

[1]Department of Physics, University of Okara, Pakistan
[2]Department of Basic Sciences, College of Veterinary and Animal Science, Jhang, Pakistan
[3]Institute of Physics, Faculty of Physical and Mathematical Sciences, The Islamia University, Bahawalpur 63100, Pakistan
[4]Department of Pathobiology, Faculty of Veterinary Sciences, Bahauddin Zakariya University Multan Pakistan
[5]Department of Clinical Medicine and Surgery, Faculty of Veterinary & Animal Sciences, The Islamia University of Bahawalpur, 63100, Pakistan
[6]Department of Zoology, The Islamia University of Bahawalpur, 63100, Pakistan
[7]Centre of Excellence in Environmental Studies, King Abdulaziz University, Jeddah, Saudi Arabia
[8]Department of Animal Nutrition and Nutritional Disease, Faculty of Veterinary Medicine, Ataturk University, Erzurum, Türkiye
[9]Faculty of Environmental Sciences, King Abdulaziz University, Jeddah, Saudi Arabia
[10]Department of Life Sciences, Western Caspian University, Baku, Azerbaijan
[11]Department of Pathology, Faculty of Veterinary & Animal Sciences, The Islamia University of Bahawalpur, 63100, Pakistan

**Corresponding authors' emails:* aroojali4088@gmail.com; dr.riaz.hussain@iub.edu.pk

Received: 28 September 2024 / Accepted: 22 January 2025 / Published Online: 06 March 2025

Abstract

Vibrating sample magnetometry (VSM), transmission electron microscopy (TEM), and X-ray diffraction (XRD) were used to characterize iron oxide nanoparticles (IONPs) synthesized via co-precipitation. TEM showed that the synthesized NPs had an average size of 13.8 nm and exhibited a saturation magnetization of 50.26 emu/gm, while XRD confirmed their crystallinity. This study assessed the toxicological impacts of IONPs on hematology, serum biochemistry, genotoxicity, and the histoarchitecture ailments in different visceral organs (liver, kidneys, spleen, brain, and heart of rabbits (*Oryctolagus cuniculus)*. A total of 16 healthy adult rabbits without infections were randomly assigned to two groups (A and B). Group A was the control whereas group B received 0.5 mg/kg bw of IONP dose once for 10 days via marginal ear vein. Visceral tissues and blood were obtained from each rabbit on days 5 and 10 of trial. The results showed a significant reduction in antioxidant enzymes and an increase in oxidative stress. The hematological profile indicated lower values of red blood cell counts, hematocrit, lymphocyte, and monocyte while significantly higher values of total white blood cell counts and neutrophil (%) in IONPs-treated rabbits. Serum biomarkers of the liver, kidneys, and heart exhibited escalated concentrations in IONPs-treated rabbits. Histopathological examination revealed notable tissue alterations like necrosis of hepatocyte, congestion, and bile duct hyperplasia in the liver, neuronal degeneration, necrosis, and microgliosis in the brain, tubular degeneration, necrosis, and congestion in the kidneys and disorganization of cardiac myofibers and edema in cardiac tissue. A significantly increased DNA damage was assessed in multiple visceral organs of treated rabbits. In conclusion, our findings demonstrate that exposure to IONPs induces toxic effects in multiple visceral organs including the kidneys, liver, spleen, heart, and brain in rabbits.

Keywords: Magnetic Oxide nanoparticles (MNPs), VSM, ROS production, Hemato-biochemistry, DNA Damage, Histopathology

How to cite this article:
Khan MS, Hussain T, Buzdar SA, Hameed MR, Ghori MT, Maheen A, Ali N, Imtiaz B, Qamar MR, Summan AS, Ali A, Iqbal R and Hussain R. Potential toxicity and mechanistic insights into organ-specific damage induced by iron oxide nanoparticles in *Oryctolagus cuniculus*. Asian J. Agric. Biol. 2025: 2024193. DOI: https://doi.org/10.35495/ajab.2024.193

Introduction

Over the last few decades, the scientific community around the world has paid huge attention to nanotechnology. Due to rapid advancement in various nanoscale chemical properties and the expansion of nanotechnology, nanoparticles (NPs) have been widely used in various industries including the manufacturing of electronic and medical devices, material sciences, public health, and food additives (Younas et al., 2024). The wide range of applications of NPs carries with it the environmental dangers and raises safety concerns (Mansour et al., 2023). The extensive use of NPs may cause risks to various target and non-target animals in several ways (Hajesmaeelzadeh et al., 2016). Previous studies have revealed that animals exposed to NPs are at tremendous risks. However, various approaches, such as oxidation state, modification, surface functionalization, and coating may reduce the potential toxicity of the NPs (Arshad et al., 2021). Due to their volatility and widespread use, NPs are routinely discharged into the environment either decisively or accidentally (Maqsood et al., 2023). Several studies have evaluated the toxicological consequences of NPs in various environmental exposures and circumstances (El-Hamaky et al., 2023). Earlier reports showed that the toxicity of different NPs depends on several factors like synthesis methods, coating, physiochemical, concentration, and physiological properties, which are vital when deciding on the use of NPs for various physiological and biomedical applications (Elbehary et al., 2023; Yew et al., 2020).

It has been recorded that various kinds of magnetic nanoparticles (MNPs) interact with living cells and induce their adverse toxic effects in terms of inhibition or promotion of catalytic activity of different enzymes. The particle-protein interaction in exposed organisms leads to malfunctioning of cells and even provokes death (Urian et al., 2021). Different studies have indicated that magnetic iron oxide NPs are preferable in the medical sciences. These are extensively used because of their excellent physiochemical characteristics and low toxicity including superparamagnetism, stability in an aqueous medium, and biocompatibility (Ali et al., 2023; Bagherzade, 2021; Hussain et al., 2022). Furthermore, it has been reported that MNPs provide a suitable platform for theragnostic and can be applied to magnetic resonance imaging (MRI) as a contrast agent in diagnostics and therapeutics in the forms of drug administration in the body, purification of proteins, bio-catalysis, and magnetic cell separation (El-Hamaky et al., 2023).

Moreover, different factors such as structure, size, shape, dosage, concentration, biodistribution, solubility, bioavailability, surface modification, immunogenicity, and pharmacokinetics of NPs play an important role in the induction of adverse toxic effects (Aslam et al., 2023; Raza et al., 2024). Therefore, it is imperative and crucial to investigate the mechanism of induction of the noxious effects of MNPs. It is also recorded that an increased surface-to-volume ratio can favor the interactions of different NPs in different body components when they enter the body via inhalation, absorption, and injection (Liu et al., 2021). The NPs may be able to cross the biological barriers of cells, and their resistance to biodegradation can enhance their adverse toxic effects (Ali et al., 2024). Therefore, monitoring and determining underlying mechanisms of induction of acute and chronic toxicity of contaminants is vital, and studies should involve the degradation of these pollutants, metabolism, defensive and inflammatory responses, and elimination from cells and different animals (Hussain et al., 2019; Hussain et al., 2024). Thus, further research is required to examine the underlying mechanisms in induction of oxidative stress, acute

and chronic toxicity, inflammatory response, defensive response, and degradation of particular products to mitigate the adverse toxic effects on public health (Saif et al., 2023; Ullah et al., 2023). However, few studies are available on the damaging effects of various forms of NPs, and still, there is a huge research gap. Animal biomedical experiments showed that MNPs were acceptable for researchers, but few studies have reported the mechanisms of induction of IONPs (Aisida et al., 2021). Therefore, this study, for the first time, determined the *in vivo* toxic effects of the IONPs on hematology, genotoxicity, serum biochemistry, and biomarkers of oxidative stress in rabbits.

Material and Methods

Chemicals and Synthesis of Nanoparticles

The material was synthesized using co-precipitation methods. At 45 °C and 450 rpm, $FeCl_3.6H_2O$ and $FeCl_2.4H_2O$ in a 2:1 ratio was mixed. By adding NH_4OH drop by drop, a pH of 9.0 was obtained. The solution was then centrifuged at 3000 rpm for half an hour to obtain the NPs (Arshad et al., 2021). After that, the NPs were dried for 7 h at 50°C in an oven. IONPs were successfully obtained by maintaining all physical and chemical operating conditions (Hajesmaeelzadeh et al., 2016; Arshad et al., 2021).

Characterizations

X-Ray Diffraction analysis

The crystalline structure of synthesized NPs was analyzed using XRD (Bruker-D8 Advance Laboratory Diffractometer, CuKα radiation, λ =1.54 Å). The XRD analysis and the Scherrer equation ($D_{hkl}= k \lambda / \beta \cos \theta$) was used to explore the phase identification, crystallinity, and particle size (Ali et al., 2023; Ali et al., 2025).

Transmission Electron Microscopy analysis

TEM was used to study the shape and size of synthesized material. The statistic histogram plot was carried out using the standard-fit tool to estimate the mean particle size (Yew et al., 2020).

Vibrating Sample Magnetometer analysis

A VSM verified the synthetic material's magnetic characteristics. According to the prior methodology, VSM (Lakeshore 7407) was used to study hysteresis loop saturation magnetization, retentivity, and coercivity (Bagherzade, 2021).

Experimental animals

Sixteen rabbits (*Oryctolagus cuniculus*) of approximately 1.5-1.6 kg body weight and almost of the same age were purchased from the local commercial market (Bahawalpur). All the experimental rabbits were housed under similar laboratory conditions. The rabbits had a free excess of fresh and clean water. The house was disinfected prior to the start of the trial. After 5 days of acclimatization, 16 rabbits were randomly divided into two groups: the untreated control (A) and the treated group (B). Group B received a 0.5 mg/kg bw of IONP dose for 10 days via a single ear vein.

Animal treatment for hematology and serum analysis

Approximately 2.5 mL of blood was obtained in an EDTA tube from the jugular vein of each NP-treated and untreated rabbit on days 5 and 10 of post-treatment for hematological analysis and serum analysis 2.5 mL of blood was obtained in a glass tube without anticoagulant from the jugular vein of each NPs-treated and untreated rabbit, and serum biochemical parameters (ALT (alanine transaminase), LDH (lactate dehydrogenase), ALP (alkaline phosphatase), AST (aspartate transaminase), creatinine, urea, cholesterol, triglycerides, and glucose) were measured using commercially available kits and previous protocol (Ghaffar et al., 2021; Hussain et al., 2020).

Biomarkers of oxidative stress and antioxidant enzymes

Malondialdehyde (MDA) was determined using the methods already described (Akram et al., 2021) in NPs-treated and untreated rabbits. Biochemical analysis of catalase (CAT), superoxide dismutase (SOD), and peroxidase (POD) was measured in the IONPs-treated and untreated organs of rabbits (Kanwal et al., 2024; Shafqat et al., 2023).

DNA damage in the liver, kidneys, and heart

DNA damage in isolated liver, kidney, and heart cells was evaluated using comet assay techniques under alkaline conditions following the established protocols (Akram et al., 2021; Hussain et al., 2019). The assay was performed with a Euromex

https://doi.org/10.35495/ajab.2024.193

fluorescence microscope (OX range; AE 3199; SL.5510; France). The frequency of DNA damage (% DNA) was determined in a total of 500 cells of each rabbit. DNA damage appeared as a diffuse "cloud" of fluorescing DNA material surrounding the nucleus or as a tail extending in the direction of the electric field (Ali et al., 2024; Hamza et al., 2023).

Gross and histopathology

The kidneys, liver, spleen, heart, and brain were carefully examined and excised from both IONPs-treated and untreated rabbits at dissection, following blood collection. A small portion of each tissue was preserved in a 10% formaldehyde solution for histological analysis. Thin sections (4-5 µm) of these organs were then prepared using a rotary microtome (Shandon Finesse, Italy). After fixation, all tissues were processed and stained using Hematoxylin and Eosin staining techniques (Hussain et al., 2018).

Statistical analysis

The data was visualized using various software tools including RadiAnt DICOM Viewer, CD DICOM Viewer, Spec Viewer, Unit Cell, Origin Pro, ImageJ, PhotoScape, and X'Pert High Score. For data analysis, IBM SPSS (version 20) was employed, using a T-test to compare the mean ± S.E. of blood, serum, and DNA damage between IONPs-treated and untreated rabbits. Statistical significance was set at $P < 0.05$ relative to the untreated group.

Results

Size and morphology analysis

Seven peaks indicated different crystal planes in XRD pattern of IONPs as shown in Figure 1 (A). The hkl values of the observed planes included (220), (311), (400), (422), (511), (440), and (533) at 2theta values of 30.4, 35.6, 43.2, 53.5, 57.1, 62.3, and 74.6.

The TEM analysis confirmed the purity of the synthesized material and showed a cubic phase in the structure. The average crystalline size of prepared NPs was 13.8 nm. The images taken from TEM analysis are shown in Figure 1(B). The statistic histogram plot is shown in Figure 1 (C), and the average grain/particle size was calculated to be 13.18 nm using the normal fit tool. VSM magnetization curves for synthesized IONPs are presented in Figure 1(D). The hysteresis loop has a 50.26 emu/gm saturation magnetization and extremely low Retentivity (Mr) and Coercivity (Hc).

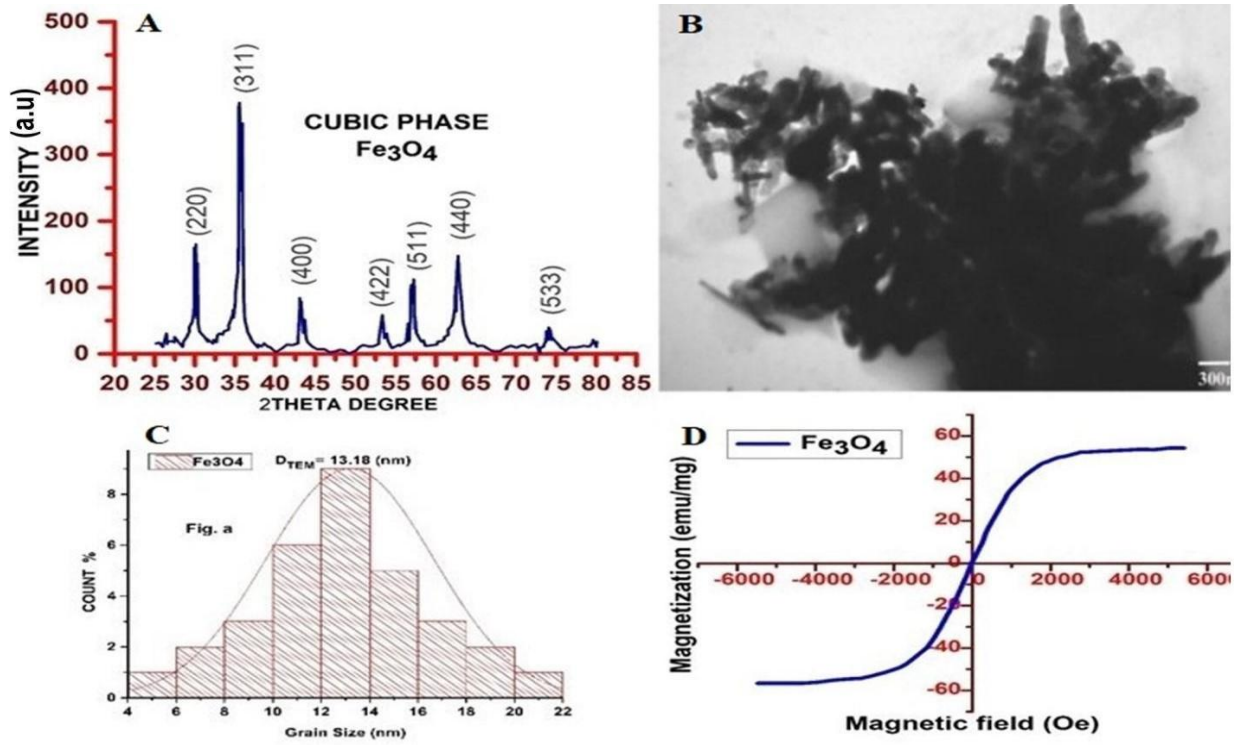

Figure 1: (A) XRD pattern of IONPs (B) TEM images of IONPs (C) Histogram plot illustrating average particle size of IONPs (D) VSM plot depicting magnetic behavior of IONPs

https://doi.org/10.35495/ajab.2024.193

Serum and hematology analysis

On days 5 and 10, rabbits treated with IONPs showed a significant reduction in red blood cells, monocytes, lymphocytes, hemoglobin, and hematocrit percentages (Figure 2), while total white blood cells and neutrophil counts were elevated.

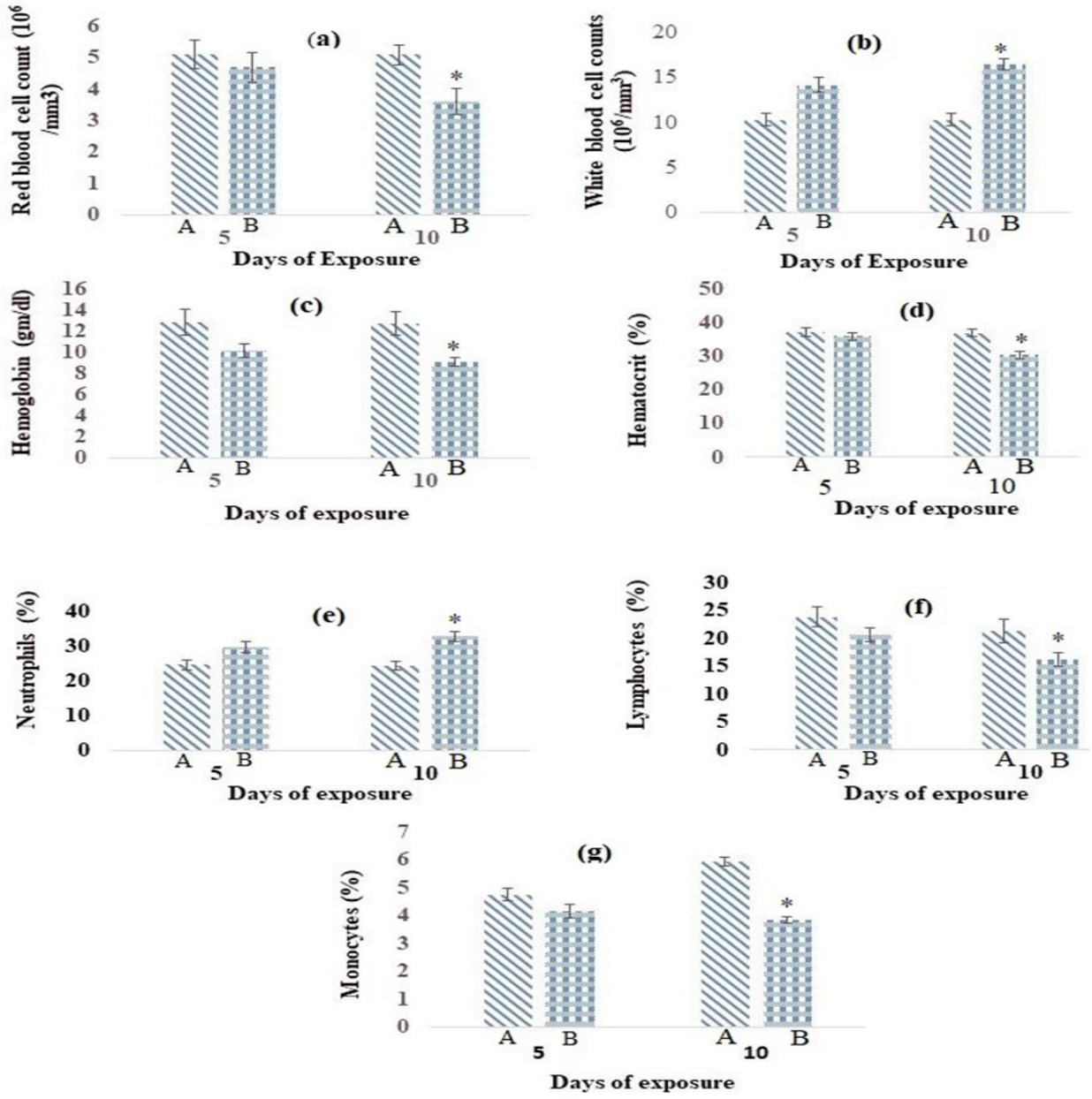

Figure-2: Photograph showing changes in blood profile of rabbits exposed to IONPs. a) red blood cell counts; b) white blood cell counts; c) hemoglobin quantity; d) hematocrit percentage; e) Neutrophil counts; f) Lymphocyte counts and g) Monocyte counts.

On day 10, total proteins and albumin levels significantly decreased in the IONPs-treated rabbits. A significant ($P < 0.05$) increase in ALT, ALP, and triglyceride levels in IONPs-treated rabbits compared to untreated ones was recorded. Serum urea, creatinine, cholesterol, and glucose levels were markedly higher in the NPs-treated group on both sampling days (Figure 3).

https://doi.org/10.35495/ajab.2024.193

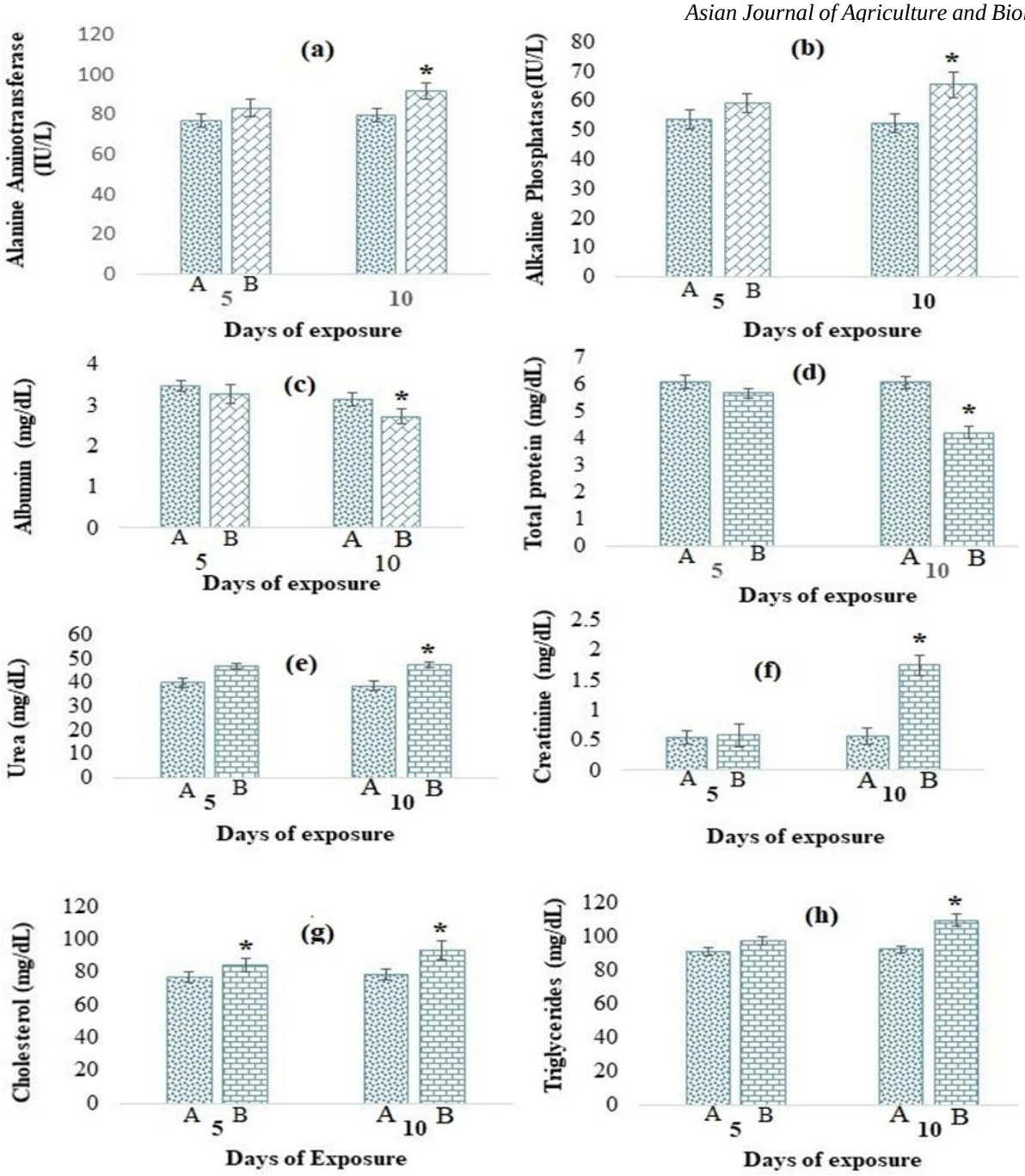

Figure-3: Photograph showing changes in serum chemistry of rabbits exposed to IONPs. a) Alanine aminotransferase; b) Alkaline phosphatase; c) Albumin quantity; d) total proteins; e) Urea concentration; f) Creatinine; g) Cholesterol and h) Triglyceride quantity.

Analysis of oxidative stress and antioxidant status

On day 10 post-exposure, the liver of rabbits treated with IONPs exhibited significantly higher biomarkers of oxidative stress compared to untreated rabbits. In the liver tissues of IONPs-treated rabbits, antioxidant enzyme including SOD, CAT, and POD showed a significant decline compared to those in untreated rabbits (Figure 4).

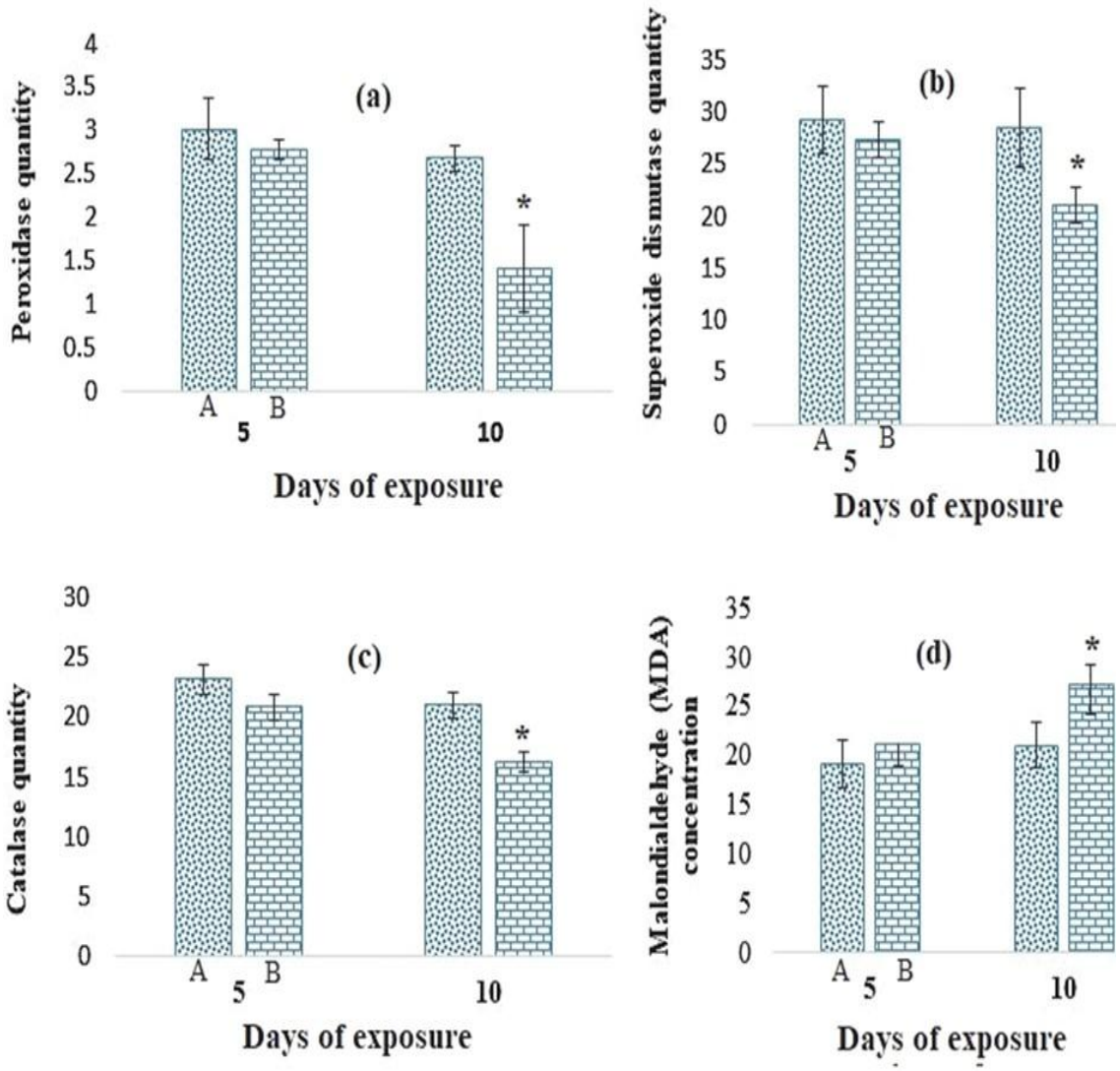

Figure-4: Photograph showing changes in oxidative stress and antioxidant enzymes chemistry of rabbits exposed to IONPs a) Peroxidase concentration; b) Superoxide dismutase quantity; c) Catalase concentrations; d) Malondialdehyde values.

Analysis of Comet Assay in liver, kidneys and heart

At day 10, the percentage of DNA damage, assessed by cell gel electrophoresis was significantly higher ($p \leq 0.05$) in isolated cells from the liver (Figure 8), kidneys, and heart of IONPs-treated rabbits in terms of increased DNA fragmentation compared to untreated group. The bar graph (Figure 5) illustrates the comparison of DNA damage (%) observed using the comet assay in untreated and IONPs-treated liver, kidneys, and heart tissues of rabbits on days 5 and 10 of experiment.

https://doi.org/10.35495/ajab.2024.193

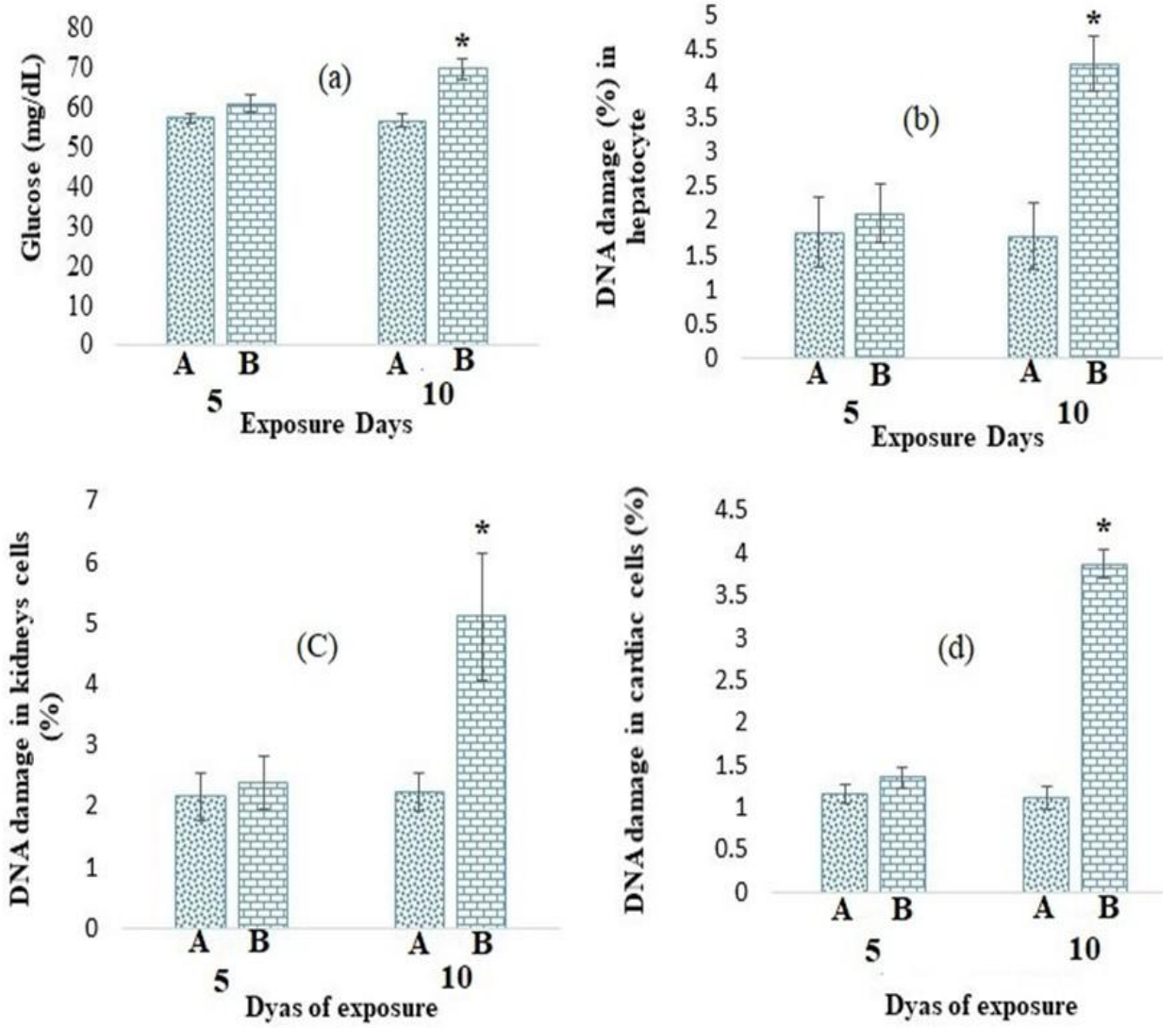

Figure-5: Photograph showing the frequency of DNA damage in; a) hepatocytes; b) isolated cells of kidneys, and c) cardiac cells of rabbits exposed to IONPs. The level of significantly difference was accepted at $P \leq 0.05$ from control group.

Microscopic analysis in visceral organs of rabbits

Kidneys: On day 5 post-IONP treatment, rabbit kidneys exhibited mild to moderate histopathological changes. However, on day 10, kidneys in IONPs-treated rabbits showed moderate to severe necrotic changes, congestion, widening of urinary spaces, renal tubular atrophy, glomerular degeneration and necrosis of renal tubules (Figure 6 A, B) and Table 1.

Liver: At day 10 of exposure, severe histopathological changes were observed in various sections of the liver of IONPs-treated rabbits. These alterations included hepatocyte necrosis, congestion, edema, hepatocyte degeneration, and atrophy (Figure 6 C, D).

https://doi.org/10.35495/ajab.2024.193

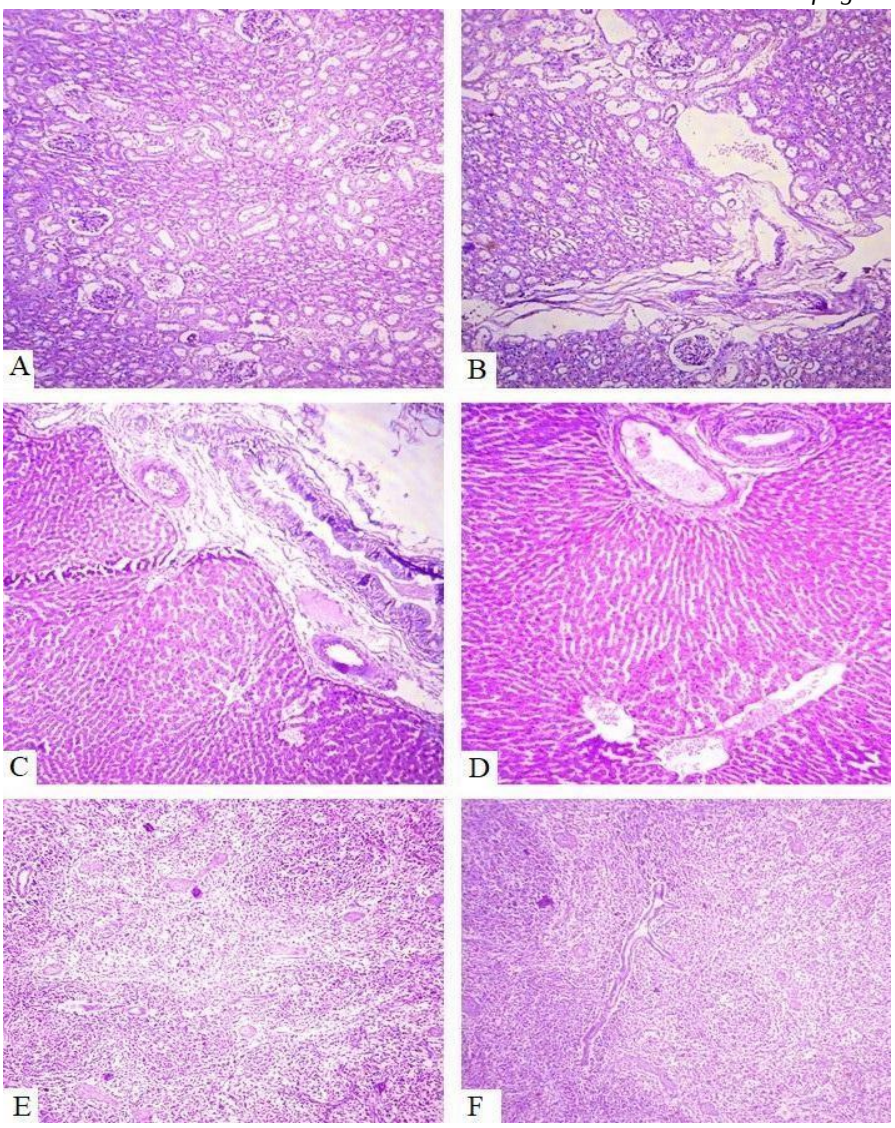

Figure-6: Photomicrograph showing severe necrosis, congestion, widening of urinary space, atrophy of renal tubule, degeneration of glomeruli and necrosis of renal tubules (A-B), necrosis of hepatocyte, congestion, edema, and degeneration of hepatocyte and congestion were observed in different sections of liver (C-D) and degeneration of white and red pulp and depletion of lymphoid (E-F) in spleen of treated rabbits. H & E Stain; 200X

Spleen: On day 5 of treatment, the spleen of IONPs-treated rabbits exhibited mild to moderate degeneration of both white and red pulp, along with lymphoid depletion (Figure 6 (E); Table 1). However, at day 10, severe histopathological changes in spleen of IONPs-treated rabbits (Figure 6 (F)) compared to those of untreated rabbits were observed.

Heart: Photomicrograph in Figure 7 (B) and Table 2 exhibit moderate to severe congestion, coagulative necrosis, edema, neutrophilic infiltration, severe myocarditis, and degeneration of cardiac myocytes in the different sections of hearts of IONPs-treated rabbits on day 10 of trial. Mild to moderate microscopic changes on day 5 (Figure 7 (A)) compared to untreated rabbits were observed.

https://doi.org/10.35495/ajab.2024.193

Brain: On day 10 post-treatment, the brains of IONPs-treated rabbits exhibited severe microscopic changes including neuronal necrosis, neuronal atrophy, microgliosis, cytoplasmic vacuolization, and congestion were observed (Figure 7 (D) and Table 2). These changes were mild to moderate (Figure 7 (C)) when compared to the untreated brain on day 5 of trial.

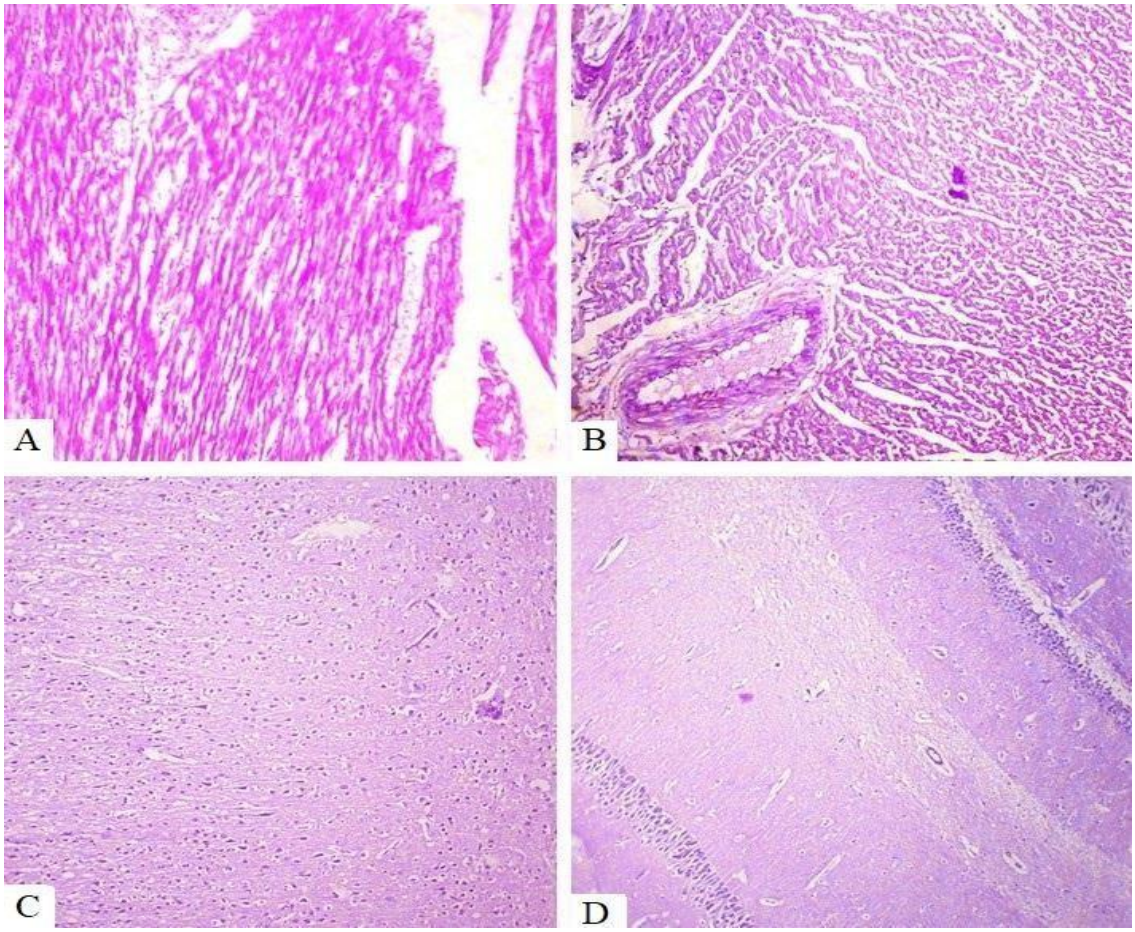

Figure-7: Photomicrograph showing congestion, coagulative necrosis, edema, neutrophilic infiltration, severe myocarditis and degeneration of cardiac myocytes (A-B) and necrosis of neurons, atrophy of neuron, microgliosis, cytoplasmic vacuolization and congestion in brain of treated rabbits (C-D). H & E Stain; 200X

Discussion

Several studies on NPs have focused on their environmental and public health impacts because of their widespread use in biomedical and biological sciences (Huang et al., 2021; Shafiq et al., 2021). Nanoparticles with diverse properties and structure are widely and frequently selected against target structures in biomedical field (Kush et al., 2021). Hence, we evaluated the toxic effects of IONPs on hematological parameters, serum biochemistry, DNA damage, and the histoarchitecture of the liver, kidneys, spleen, brain, and heart of rabbits (Oryctolagus cuniculus). XRD analysis of IONPs revealed multiple Bragg reflection peaks. The reported scattering angles and their corresponding hkl values confirmed the purity of the crystallographic structure of the cubic phase IONPs, which were in agreement with the previous research (Basavegowda et al., 2016). The TEM images showed the average particle size of prepared NPs. The hysteresis loop's almost zero Retentivity (Mr) and Coercivity (Hc) proved the supermagnetic behavior of IONPs. The prepared IONPs are suitable for MRI due to their 50.26 emu/gm saturation magnetization (Ms) as reported in earlier studies (Besenhard et al., 2021; van Zandwijk et al., 2021). In treated rabbits, red blood cells,

https://doi.org/10.35495/ajab.2024.193

hemoglobin, and hematocrit values were reduced and total leukocytic count and neutrophils were increased. Lower blood values may be attributed to the noxious impact of IONPs on the bone marrow, whereas higher white blood cell and neutrophil numbers may be due to injurious/harmful stimuli and the generation of free radicals (Couto et al., 2014; Ali et al., 2024). The increased biomarkers of renal function tests, liver function tests, and cardiac biomarkers in our study could be due to hepatic, renal, and cardiac damage (Hussain et al., 2018; Qiao et al., 2021). Previous studies have found increased oxidative stress, free radical production, and hepatic lipid peroxidation (Ghaffar et al., 2021; Kalsoom et al., 2024; Nwafili and Uchechi-Ibinabo, 2023).

Previous studies involving intravenous administration of polyacrylic acid-coated IONPs in mice have demonstrated an increase in cardiac indicators such as creatine kinase (Couto et al., 2014). Previously similar to our results on hematology, an increase in lymphocyte counts, blood cell counts, and goblet cells in the intestinal tissue of fish treated with iron salts and Fe_3O_4 NPs have been recorded (Malhotra et al., 2020).

IONP treatment led to a significant increase in oxidative stress and a marked depletion of antioxidant biomarkers. Earlier studies have shownthat fish and rabbits exposed to low concentrations of cobalt ferrite nanoparticles exhibited reduced catalase activity alongside elevated levels of acid phosphatase, glutathione S-transferase, and other indicators of oxidative stress (Ahmad et al., 2015; Khan et al., 2023). Mitochondrial respiration anomalies in rabbit tissues may be the reasons for oxidative stress and antioxidant disorders in our study (Saoudi et al., 2020). Previously, enhanced lipid peroxidation along with ROS in muscles of rat (Malhotra et al., 2020) and fish (Ahmad et al., 2015) has also been recorded. IONPs exposure may enhance DNA damage in hepatocytes, cardiac myocytes, and kidney cells at day 10 due to NF-kB activation, which causes oxidative stress and DNA fragmentation (Ahmad et al., 2015; Khan et al., 2022). In addition, NP-induced cytotoxicity in exposed cells has been linked to redox homeostasis disruption and Bax/Bcl-2 pathway changes (Mohammadinejad et al., 2019; Cem et al., 2024).

The remarkable increased DNA damage in livers, hearts, and kidneys of treated rabbits may be due to oxidative stress (Hussain et al., 2022). Recent studies have shown that IONPs generate free radicals, induce lipid peroxidative stress, deplete antioxidant enzymes, and enhance caspase-3 and caspase-9 activity in exposed cells, causing genotoxicity (Khan et al., 2022; Özüiçli et al., 2023).The higher DNA damage frequency may potentially be due to protein carbonylation as well as ubiquitin conjugate abnormalities (Malhotra et al., 2020; Hussain et al., 2022) and abnormal cytosolic calcium in tissues (Lin et al., 2014; Ran et al., 2015; Ullah et al., 2023).

Figure-8: Photomicrograph showing DNA-damaged material fluorescing around the nucleus in isolated cells from the liver of rabbits exposed to IONPs. Ethidium bromide stain; 400X.

In IONPs-treated rabbits, different histological abnormalities observed in our study including hepatocyte degeneration, congestion, edema, and necrosis have also been reported (El-Bahr et al., 2021). The rapid increase of oxidative stress may activate archetypal AhR-regulated genes (Cyp1a1, Nqo1 mRNA, and Cyp1b1) in hepatocytes, causing nuclear localization and these symptoms in treated animals (Elshenawy and El-Kadi, 2015; Qiao et al., 2021). The rapid production of free radicals which release apoptotic signals from mitochondrial membranes may also cause liver parenchyma necrosis in NPs-treated rabbits (Akram et al., 2021). The toxic effect of Fe_3O_4 NPs on rabbits is little documented. Various investigations have also found abnormal alterations in the liver of rats (Su et al., 2018) and rabbits (Bai et al., 2020) and, unlike other animals, due to exposure to these NPs (Ma et al., 2012; Murali et al., 2018; Wu and Tang, 2018). In rats, sub-lethal quantities of oleate-coated IONPs caused sinusoid space expansion, lipidosis, and necrosis in liver tissues (Awaad and Seleem, 2016).

Also, IONPs-treatment has little influence on cell viability, apoptosis, along with oxidative stress. (Mejías et al., 2013). Our study found microscopic abnormalities in IONPs-treated kidneys of rabbits due to histone acetylation and DNA methylation, increased IL-8 production, and promoter abnormalities. Previously, no IONPS-induced renal pathology has been reported in mice (Couto et al., 2014). The modification of CpG may also cause dysregulation as well as cell migratory abilities that favor kidney damage (Singh et al., 2015). Previously, NPs-exposed kidneys of animals showed tubular epithelial cell degeneration, congestion, necrosis, as well as hemorrhages (Abdel-Latif et al., 2021;Shahid et al., 2023). Under a light microscope, the spleen of treated rabbits showed cell depletion and white and red pulp degeneration. Earlier, MNP-exposed animals had no histological spleen changes (Aslam et al., 2023). IONPs may cause histological alterations in the spleen of rabbits by inducing oxidative stress. NPs have been shown to induce oxidative stress and lipid peroxidation in mice (Couto et al., 2014). Histopathological abnormalities in visceral tissues may be due to protein (TNF-R2 and caspase 3) over-release (Awaad and Aziz, 2021; Awaad and Seleem, 2016; Teng et al., 2021). The microscopic abnormalities in our study may also be linked to increased connective tissue growth factors and collagen fiber proteins after day 10 of treatment. According to studies, NPs are unable to penetrate the blood-brain barrier (Couto et al., 2014). Research indicates that the blood-brain barrier prevents passive diffusion of large-molecule neurotherapeutics and 98% of small-molecule medicines due to tight junction gaps. In our work, IONPs rapidly produced free radicals (hydrogen peroxide and reactive oxygen species), which may have caused microscopic brain tissue abnormalities. In IONPs-treated rabbits, microscopic cardiac changes may be linked to inflammatory mediator release and reactive oxygen species formation (Couto et al., 2014; Freitas et al., 2009; Ma et al., 2012).

Conclusion

In conclusion, this study demonstrates that the synthesized IONPs, characterized by a size of 13.8 nm and a saturation magnetization of 50.26 emu/gm, exhibit significant toxic effects on various visceral organs in rabbits. The alterations observed in hematological and serum biochemical profiles indicate potential organ dysfunction, accompanied by increased oxidative stress and DNA damage. Histopathological analyses further highlight the detrimental effects on tissue integrity, particularly in the liver, brain, kidneys, and heart. These findings emphasize the critical need for comprehensive investigations into the safety and potential health risks of IONPs in biomedical applications, underscoring the necessity of understanding their toxicological profiles to ensure their safe and effective use in clinical contexts.

Disclaimer: None
Source of Funding: None
Conflicts of Interest: None

Data Availability Statement

When needed, the author can provide experiment data.

Contribution of Authors

Khan MS, Buzdar SA, Hussain R, Ghori MT & Ali A: Conceived idea, conducted the research, collected, analyzed and interpreted the results. Qamar MR and Summan AS & Iqbal R: Edited and approved the final draft of the article.
Hussain T, Imtiaz B, Hameed MR, Maheen A & Ali N: Involved in preparation of initial draft.

References

Abdel-Latif HM, Shukry M, Euony OIE, Mohamed Soliman M, Noreldin AE, Ghetas HA, Dawood MA and Khallaf MA, 2021. Hazardous Effects of SiO2 Nanoparticles on Liver and Kidney Functions, Histopathology Characteristics, and Transcriptomic Responses in Nile Tilapia (Oreochromis niloticus) Juveniles. Biology. 10: 183.

Ahmad F, Liu X, Zhou Y and Yao H, 2015. An in vivo evaluation of acute toxicity of cobalt ferrite (CoFe2O4) nanoparticles in larval-embryo Zebrafish (Danio rerio). Aquat. Toxicol. 166: 21-28.

Aisida SO, Ali A, Oyewande OE, Ahmad I, Ul-Hamid A, Zhao T-k, Maaza M and Ezema FI, 2021. Biogenic synthesis enhanced structural, morphological, magnetic and optical properties of zinc ferrite nanoparticles for moderate hyperthermia applications. J. Nanoparticle Res. 23: 1-14.

Akram R, Iqbal R, Hussain R, Jabeen F and Ali M, 2021. Evaluation of oxidative stress, antioxidant enzymes and genotoxic potential of bisphenol A in fresh water bighead carp (Aristichthys nobils) fish at low concentrations. Environmental pollution. 268: 115896.

Ali A, Saeed S, Hussain R, Afzal G, Siddique AB, Parveen G, Hasan M and Caprioli G, 2023. Synthesis and characterization of silica, silver-silica, and zinc oxide-silica nanoparticles for evaluation of blood biochemistry, oxidative stress, and hepatotoxicity in albino rats. ACS omega. 8: 20900-20911.

Ali A, Saeed S, Hussain R, Saif MS, Waqas M, Asghar I, Xue X and Hasan M, 2024. Exploring the impact of silica and silica-based nanoparticles on serological parameters, histopathology, organ toxicity, and genotoxicity in Rattus norvegicus. Applied Surface Science Advances. 19: 100551.

Ali A, Ali SR, Hussain R, Anjum R, Liu Q, Elshikh MS, Alkubaisi N, Iqbal R, Tabor S and Gancarz M. Comparative study of silica and silica-decorated ZnO and ag nanocomposites for antimicrobial and photocatalytic applications. Sci. Rep. 15 :5010.

Arshad JM, Raza W, Amin N, Nadeem K, Arshad MI and Khan MA, 2021. Synthesis and characterization of cobalt ferrites as MRI contrast agent. Materials Today: Proceedings. 47: S50-S54.

Aslam N, Ali A, Sial B, Maqsood R, Mahmood Y, Mustafa G and Sana A, 2023. Assessing the dual impact of zinc oxide nanoparticles on living organisms: Beneficial and noxious effects. Int. J. Agri. Biosc. 12: 267-276.

Awaad A and Aziz HOA, 2021. Iron biodistribution profile changes in the rat spleen after administration of high-fat diet or iron supplementation and the role of curcumin. J. Mol. Histol. 1-16.

Awaad A and Seleem A, 2016. Histochemical changes in neonatal liver caused by vaginal instillation of magnetic nanoparticles in pregnant mice. Biotech. Histochem. 91: 48-62.

Bagherzade G, 2021. The anchoring of a Cu (ii)–salophen complex on magnetic mesoporous cellulose nanofibers: green synthesis and an investigation of its catalytic role in tetrazole reactions through a facile one-pot route. RSC adv. 11: 19203-19220.

Bai C, Hu P, Liu N, Feng G, Liu D, Chen Y, Ma M, Gu N and Zhang Y, 2020. Synthesis of Ultrasmall Fe3O4 Nanoparticles as T 1–T 2 Dual-Modal Magnetic Resonance Imaging Contrast Agents in Rabbit Hepatic Tumors. ACS Appl. Nano Mater. 3: 3585-3595.

Basavegowda N, Mishra K, Lee YR and Joh YG, 2016. Magnetically separable iron oxide nanoparticles: an efficient and reusable catalyst for imino Diels–Alder reaction. Bull. Korean Chem. Soc. 37: 142-147.

Besenhard MO, Panariello L, Kiefer C, LaGrow AP, Storozhuk L, Perton F, Begin S, Mertz D, Thanh NTK and Gavriilidis A, 2021. Small iron oxide nanoparticles as MRI T 1 contrast agent: scalable inexpensive water-based synthesis using a flow reactor. Nanoscale. 13: 8795-8805.

Cem Ö, Yildiz B, Demirel R and Özden Ö, 2024. Effects of zinc oxide nanoparticles on pyruvate dehydrogenase and lactate dehydrogenase expressions and apoptotic index in breast cancer cells. Kafkas Univ Vet Fak Derg, 30: 489-496

Couto D, Freitas M, Vilas-Boas V, Dias I, Porto G, Lopez-Quintela MA, Rivas J, Freitas P, Carvalho F and Fernandes E, 2014. Interaction of polyacrylic acid coated and non-coated iron oxide nanoparticles with human neutrophils. Toxicol. Lett. 225: 57-65.

El-Bahr SM, Elbakery AM, El-Gazzar N, Amin AA, Al-Sultan S, Alfattah MA, Shousha S, Alhojaily S, Shathele M and Sabeq II, 2021. Biosynthesized iron oxide nanoparticles from Petroselinum crispum leaf extract mitigate lead-acetate-induced anemia in male albino rats: hematological, biochemical and histopathological features. Toxics. 9: 123.

El-Hamaky AM, Hassan AA, Wahba AK and El-Mosalamy MM, 2023. Influence of copper and zinc nanoparticles on genotyping characterizations of multi-drug resistance genes for some calf pathogens. Int. J. Vet. Sci. 12: 309–317.

Elbehary M, Dowidar YA, Ashour AM, El-Fattah EMA and Monir A, 2023. Effect of in vitro maturation medium supplementation with chitosan nanoparticles on the river buffalo cumulus-oocyte complexes. Int. J. Vet. Sci. 12:341–346.

Elshenawy OH and El-Kadi AO, 2015. Modulation of aryl hydrocarbon receptor-regulated enzymes by trimethylarsine oxide in C57BL/6 mice: In vivo and in vitro studies. Toxicol. Lett. 238: 17-31.

Freitas M, Lima JL and Fernandes E, 2009. Optical probes for detection and quantification of neutrophils' oxidative burst. A review. Anal. Chim. Acta. 649: 8-23.

Ghaffar A, Hussain R, Abbas G, Khan R, Akram K, Latif H, Ali S, Baig S, Du X and Khan A, 2021. Assessment of genotoxic and pathologic potentials of fipronil insecticide in Labeo rohita (Hamilton, 1822). Toxin Rev. 40: 1289-1300.

Ghaffar A, Hussain R, Ahmad N, Ghafoor R, Akram MW, Khan I and Khan A, 2021. Evaluation of hemato-biochemical, antioxidant enzymes as biochemical biomarkers and genotoxic potential of glyphosate in freshwater fish (Labeo rohita). Chem. Ecol. 37: 646-67.

Hajesmaeelzadeh F, Shanehsazzadeh S, Grüttner C, Daha FJ and Oghabian MA, 2016. Effect of coating thickness of iron oxide nanoparticles on their relaxivity in the MRI. Iran. J. Basic Med. Sci. 19: 166.

Hamza RMA, Aslam H, Aleem K, Bukhari MA, Nadeem J, Farooq H, Akbar M, Manzoor M and Ashraf H, 2023. The genetics of insecticide resistance in relation to climate change. Agrobiol. Rec. 12: 92-98.

Huang H, Feng W and Chen Y, 2021. Two-dimensional biomaterials: material science, biological effect and biomedical engineering applications. Chem. Soc. Rev. 50: 11381-11485.

Hussain R, Ali F, Rafique A, Ghaffar A, Jabeen G, Rafay M, Liaqat S, Khan I, Malik R and Khan MK, 2019. Exposure to Sub-Acute Concentrations of Glyphosate Induce Clinico-Hematological, Serum Biochemical and Genotoxic Damage in Adult Cockerels. Pak. Vet. J. 39: 181-186.

Hussain R, Ghaffar A, Abbas G, Jabeen G, Khan I, Abbas RZ, Noreen S, Iqbal Z, Chaudhary IR and Ishaq HM, 2020. Thiamethoxam at sublethal concentrations induces histopathological, serum biochemical alterations and DNA damage in fish (Labeo rohita). Toxin Reviews1-11.

Hussain R, Ghaffar A, Abbas G, Jabeen G, Khan I, Abbas RZ, Noreen S, Iqbal Z, Chaudhary IR and Ishaq HM, 2022. Thiamethoxam at sublethal concentrations induces histopathological, serum biochemical alterations and DNA damage in fish (Labeo rohita). Toxin. Rev. 41: 154-164.

Hussain R, Ghaffar A, Ali HM, Abbas RZ, Khan JA, Khan IA, Ahmad I and Iqbal Z, 2018. Analysis of different toxic impacts of Fipronil on growth, hemato-biochemistry, protoplasm and reproduction in adult cockerels. Toxin. Rev. 37: 294-303.

Hussain R, Naz S, Alam S, Ali HM, Ali A, Khan MS, Fouad D, Ataya FS, Mammadov A and Li K, 2024. Temporal and dosage impact of magnesium oxide nanoparticles on grass carp: unveiling oxidative stress, DNA damage, and antioxidant suppression. Toxicol. Mech. Methods. 35: 19-31.

Kalsoom R, Asfour HZ, Ali HM, Qayyum A, Anjum S, Maqbool F, Sial N, Hussain R, Alamri SH, Ali N, Rajeh N, Irshad I and Idrees A. Bifenthrin induced toxic effects on haematological, reproductive histo-morphological profile in adult male quail (Coturnix japonica). Asian J. Agric. Biol. 2024: 2023357.

Kanwal N, Aziz S, Abdullah S, Ali MS and Ahmad N, 2024. Studies on the changes in antioxidant enzyme activity induced by parathion in Hypophthalmichthys molitrix. Continental. Vet. J. 4: 40-45.

Kush P, Kumar P, Singh R and Kaushik A, 2021. Aspects of high-performance and bio-acceptable magnetic nanoparticles for biomedical application. Asian J. Pharm. Sci.16: 704-737.

Khan MS, Buzdar SA, Hussain R, Alouffi A, Aleem MT, Farhab M, Javid MA, Akhtar RW, Khan I, Almutairi MM, 2023. Cobalt Iron Oxide (CoFe2O4) Nanoparticles Induced Toxicity in Rabbits. Vet. Sci. 10: 514

Khan MS, Buzdar SA, Hussain R, Afzal G, Jabeen G, Javid MA, Iqbal R, Iqbal Z, Mudassir KB, Saeed S, Rauf A and Ahmad H.I 2022. Hematobiochemical, Oxidative Stress, and Histopathological Mediated Toxicity Induced by Nickel Ferrite (NiFe2O4) Nanoparticles in Rabbits. Oxid. Med. Cell. Longev. 2022: 5066167.

Lin Y-R, Kuo C-J, Lin HY-H, Wu C-J and Liang S-S, 2014. A proteomics analysis to evaluate cytotoxicity in nrk-52e cells caused by unmodified nano-fe3o4. Sci. World J. 2014: 754721.

Liu B, Zeng Q, Chen H, Liao J, Bai Y, Han Q, Qiao N, Wang S, Mehmood K and Hussain R, 2021. The hepatotoxicity of altrazine exposure in mice involves the intestinal microbiota. Chemosphere. 272: 129572.

Ma P, Luo Q, Chen J, Gan Y, Du J, Ding S, Xi Z and Yang X, 2012. Intraperitoneal injection of magnetic Fe3O4-nanoparticle induces hepatic and renal tissue injury via oxidative stress in mice. Int. J. Nanomed. 7: 4809.

Malhotra N, Lee J-S, Liman RAD, Ruallo JMS, Villaflores OB, Ger T-R and Hsiao C-D, 2020. Potential toxicity of iron oxide magnetic nanoparticles: A review. Molecules. 25: 3159.

Mansour MK, Yousif HM, Rezk RAESA and El Mahdy AM, 2023. Promotives of Nano-Zinc Oxide as an Immune Stimulant in the Treatment of Lambs Suffering from Zinc Deficiency. Kafkas. Univ. Vet. Fak. Derg. 29: 183-190

Maqsood R, Ali A, Sial BE, Aslam N, Mehmood Y, Mustafa G, Sohail T and Farhab M, 2023. In vivo and in vitro genotoxic effects of Zinc Oxide Nanoparticles (ZnO NPs): A comprehensive review. Continental Vet. J. 3:1-14

Mejías R, Gutiérrez L, Salas G, Pérez-Yagüe S, Zotes TM, Lázaro FJ, Morales MP and Barber DF, 2013. Long term biotransformation and toxicity of dimercaptosuccinic acid-coated magnetic nanoparticles support their use in biomedical applications. J. Control. Release. 171: 225-233.

Mohammadinejad R, Moosavi MA, Tavakol S, Vardar DÖ, Hosseini A, Rahmati M, Dini L, Hussain S, Mandegary A and Klionsky DJ, 2019. Necrotic, apoptotic and autophagic cell fates triggered by nanoparticles. Autophagy. 15: 4-33.

Murali M, Athif P, Suganthi P, Bukhari AS, Mohamed HS, Basu H and Singhal R, 2018. Toxicological effect of Al2O3 nanoparticles on histoarchitecture of the freshwater fish Oreochromis mossambicus. Environ. Toxicol. Pharmacol. 59: 74-81.

Nwafili S and Uchechi-Ibinabo J, 2023. Survey of catfish hatchery knowledge and practices in Obio-Akpor local government area, Rivers State, Nigeria. Agrobiol. Rec. 13: 61-69.

Özüiçli M, Girişgin AO, Diker Aİ, Baykalır Y, Kısadere İ and Aydın L, 2023. The efficacy of thyme, peppermint, eucalyptus essential oils and nanoparticle ozone on nosemosis in honey bees. Kafkas. Univ. Vet. Fak. Derg. 29: 335-342.

Qiao N, Yang Y, Liao J, Zhang H, Yang F, Ma F, Han Q, Yu W, Li Y and Hu L, 2021. Metabolomics and transcriptomics indicated the molecular targets of copper to the pig kidney. Ecotoxicol. Environ. Saf. 218: 112284.

Ran Q, Xiang Y, Liu Y, Xiang L, Li F, Deng X, Xiao Y, Chen L, Chen L and Li Z, 2015. Eryptosis indices as a novel predictive parameter for biocompatibility of Fe 3 O 4

magnetic nanoparticles on erythrocytes. Sci. Rep. 5: 1-15.

Raza A, Saleem MI, Hussain SF, Mahfooz A, Saleemi MK, Ashar A, Zafar K, Ahmad A, Zaka F, Butt AA, Shah SKD, Kaleem QM, Mustafa S, Sultan T, Rehman A, Hassan B and Saleem MW, 2024. Comparative effectiveness of calcium zincate nanocomposite and zinc oxide nanoparticles as healing agent against third degree burn wound in rabbits. Continental Vet. J. 4: 231-240.

Saif MS, Hasan M, Zafar A, Ahmed MM, Tariq T, Waqas M, Hussain R, Zafar A, Xue H and Shu X, 2023. Advancing nanoscale science: synthesis and bioprinting of zeolitic imidazole framework-8 for enhanced anti-infectious therapeutic efficacies. Biomedicines. 11: 2832.

Shahid A, Faizan M and Raza MA, 2023. Potential role of silver nanoparticles (AgNPs) and zinc nanoparticles (ZnNPs) for plant disease management. Agrobiol. Rec. 14: 59-69.

Saoudi M, Rahmouni F, El Aroui M, Boudaya M, Jamoussi K, Kallel C and El Feki A, 2020. Ameliorative effects of Urtica dioica aqueous extract against hepatotoxicity and nephrotoxicity induced by insecticide mixture in adult male rats. Entomology and Applied Science Letters. 7: 98-110.

Shafiq T, Uzair M, Iqbal MJ, Zafar M, Hussain SJ and Shah SAA, 2021. Green Synthesis of Metallic Nanoparticles and Their Potential in Bio-Medical Applications. Nano. Biomed. Eng. 13: 191-206.

Shafqat S, Abbass J, Khan A, Afsheen H, Afzal G, Nisa QU, Alam S, Shamsher MI and Jamal A, 2023. Oxidative stress and toxicological impacts of Ethoxysulfuron exposure on bone marrow, and intestinal morphometry in male Japanese Quail. Continental. Vet. J. 3: 78-85.

Singh RD, Tiwari R, Khan H, Kumar A and Srivastava V, 2015. Arsenic exposure causes epigenetic dysregulation of IL-8 expression leading to proneoplastic changes in kidney cells. Toxicol. Lett. 237: 1-10.

Su H, Song X, Li J, Iqbal MZ, Kenston SSF, Li Z, Wu A, Ding M and Zhao J, 2018. Biosafety evaluation of Janus Fe3O4-TiO2 nanoparticles in Sprague Dawley rats after intravenous injection. Int. J. Nanomed. 13: 6987.

Teng C, Jiang C, Gao S, Liu X and Zhai S, 2021. Fetotoxicity of Nanoparticles: Causes and Mechanisms. Nanomater. 11: 791.

Ullah A, Al-Saeed FA, Abduallah AM, Ahmed AE, Shahzad A, Amjad N, Ali A, Mostafa MS and Hussain R, 2023. Calcium Nanoparticles Induce Oxidative Stress in Erythrocytes, Neurotoxicity and Toxicity in Albino Rats (Rattus norvegicus). Pak. Vet. J. 43: 241-247.

Urian Y, Atoche-Medrano J, Quispe LT, Félix LL and Coaquira J, 2021. Study of the surface properties and particle-particle interactions in oleic acid-coated Fe3O4 nanoparticles. J. Magn. Magn. Mater. 525: 167686.

van Zandwijk JK, Simonis FF, Heslinga FG, Hofmeijer EI, Geelkerken RH and Ten Haken B, 2021. Comparing the signal enhancement of a gadolinium based and an iron-oxide based contrast agent in low-field MRI. PloS One. 16: e0256252.

Wu T and Tang M, 2018. Review of the effects of manufactured nanoparticles on mammalian target organs. J. Appl. Toxicol. 38: 25-40.

Yew YP, Shameli K, Mohamad SE, Lee KX and Teow S-Y, 2020. Green synthesized montmorillonite/carrageenan/Fe3O4 nanocomposites for pH-responsive release of protocatechuic acid and its anticancer activity. Int. J. Mol. Sci. 21: 4851.

Younas K, Khan RAA, Numan A, Ali H, Elahi A, Khan A, Zahid R, Saeed H, Iqbal K and Huzaifa MA, 2024. . Effect of metallic and nonmetallic nanoparticles (NPs) and their salts in reproductive biotechnology. Continental.Vet. J. 4: 110-119.